

# Elucidation of Piericidin A1 Biosynthetic Locus Revealed a Thioesterase-Dependent Mechanism of $\alpha$ -Pyridone Ring Formation

Qian Liu,<sup>1,2</sup> Fen Yao,<sup>1</sup> Yit Heng Chooi,<sup>2</sup> Qianjin Kang,<sup>1</sup> Wei Xu,<sup>2</sup> Yanran Li,<sup>2</sup> Yucheng Shao,<sup>1</sup> Yuefeng Shi,<sup>4</sup> Zixin Deng,<sup>1</sup> Yi Tang,<sup>2,3,\*</sup> and Delin You<sup>1,\*</sup>

<sup>1</sup>State Key Laboratory of Microbial Metabolism and School of Life Sciences and Biotechnology, Shanghai Jiao Tong University, Shanghai 200030, China

<sup>2</sup>Department of Chemical and Biomolecular Engineering

<sup>3</sup>Department of Chemistry and Biochemistry

University of California, Los Angeles, CA 90095, USA

<sup>4</sup>Institute of Plant Protection and Microbiology, Zhejiang Academy of Agricultural Sciences, Hangzhou 310021, China

\*Correspondence: dlyou@sjtu.edu.cn (D.Y.), yitang@ucla.edu (Y.T.)

DOI 10.1016/j.chembiol.2011.12.018

## SUMMARY

Piericidins are a class of  $\alpha$ -pyridone antibiotics that inhibit mitochondrial respiratory chain and exhibit antimicrobial, antifungal, and antitumor activities. Sequential analysis of *Streptomyces piomogeues* var. *Hangzhouwanensis* genome revealed six modular polyketide synthases, an amidotransferase, two methyltransferases, and a monooxygenase for piericidin A1 production. Gene functional analysis and deletion results provide overview of the biosynthesis pathway. Furthermore, in vitro characterization of the terminal polyketide synthase module with the thioesterase domain using  $\beta$ -ketoacyl substrates was performed. That revealed a pathway where the  $\alpha$ -pyridone ring formation is dependent on hydrolysis of the product  $\beta$ ,  $\delta$ -diketo carboxylic acid by the C-terminal thioesterase followed by amidation and cyclization. These findings set the stage to investigate unusual enzymatic mechanisms in  $\alpha$ -pyridone antibiotics biosynthesis, provide a foundation for genome mining of  $\alpha$ -pyridone antibiotics, and produce analogs by molecular engineering.

## INTRODUCTION

Piericidins belong to a family of  $\alpha$ -pyridone antibiotics that are produced predominantly by various *Streptomyces* species. This growing family of natural products was grouped according to different side chains. Piericidin A1 (**1**) (Figure 1) was first isolated from *Streptomyces mobaraensis* in the late 1950s, later from *Streptomyces piomogeues* var. *Hangzhouwanensis*, and recently from a symbiotic *Streptomyces* of beewolf digger wasps (Kroiss et al., 2010). Because of its high structural similarity to ubiquinone (Figure 1), **1** exhibits important biological activities, which include potent inhibitory activity toward mitochondrial NADH dehydrogenase (complex I,  $K_i = 0.6\text{--}1.0\ \mu\text{M}$ ) by competing with ubiquinone (Gutman et al., 1970). Besides NADH dehydro-

genase, glucose transporter has also been identified as the functional target of glucopiericidin A (Matsumoto et al., 1987) by metabolomic analysis (Kitagawa et al., 2010). **1** shows diverse antibacterial and antifungal activities with a minimum inhibitory concentration as low as 6  $\mu\text{g/ml}$ , and it can selectively kill some insects at a concentration as low as 4.8  $\mu\text{g/ml}$  (Hall et al., 1966). Furthermore, **1** was identified as a highly selective antitumor agent in animal model (Hwang et al., 2008).

**1** is a prototypical member of the rare subclass of  $\alpha$ -pyridone natural products, which has attracted much interest from the biosynthesis viewpoint. The structure of **1** was elucidated by nuclear magnetic resonance (NMR) investigation (Takahashi et al., 1965) and consists of an  $\alpha$ -pyridone ring attached to an unsaturated linear polyketide chain. The total chemical synthesis of **1** has been achieved successfully (Lipshutz and Amorelli, 2009; Schnermann and Boger, 2005; Schnermann et al., 2006), but the studies on the biosynthesis of **1** are limited (Tanabe and Seto, 1970). The previous isotope-feeding experiment showed that the carbon backbone of **1** is derived from four molecules of acetate and five molecules of propionate, while the incorporation of <sup>15</sup>N-labeled aspartate and serine was low.

Apart from **1**, the biosynthesis of other  $\alpha$ -pyridone antibiotics has been investigated as well. The isotope-feeding experiment in studying the biosynthesis of iromycin (Figure 1) revealed that acetate and propionate are the carbon precursors and that <sup>15</sup>N from ammonium sulfate can be successfully incorporated into the  $\alpha$ -pyridone ring (Surup et al., 2007). This is in contrast to the biosynthesis of the other well-studied  $\alpha$ -pyridone antibiotics, such as kirromycin (Figure 1), that use the hybrid polyketide synthase-nonribosomal peptide synthetase (PKS-NRPS) pathway to incorporate  $\beta$ -alanine into the  $\alpha$ -pyridone ring (Weber et al., 2008). The fungal  $\alpha$ -pyridone natural products well known for their neurotogenic activity (Jessen et al., 2011), such as tenellin (Eley et al., 2007) and aspyridone (Bergmann et al., 2007), are each biosynthesized by an iterative PKS-NRPS system and modified with a cytochrome P450 oxidase (Halo et al., 2008).

In this report, we have sequenced and identified a biosynthetic gene cluster of **1** from *S. piomogeues* var. *Hangzhouwanensis*. Bioinformatic analysis of the gene cluster, in vivo gene replacement, and in vitro characterization of the terminal PKS module led to a proposed biosynthetic pathway of **1**. The role of the

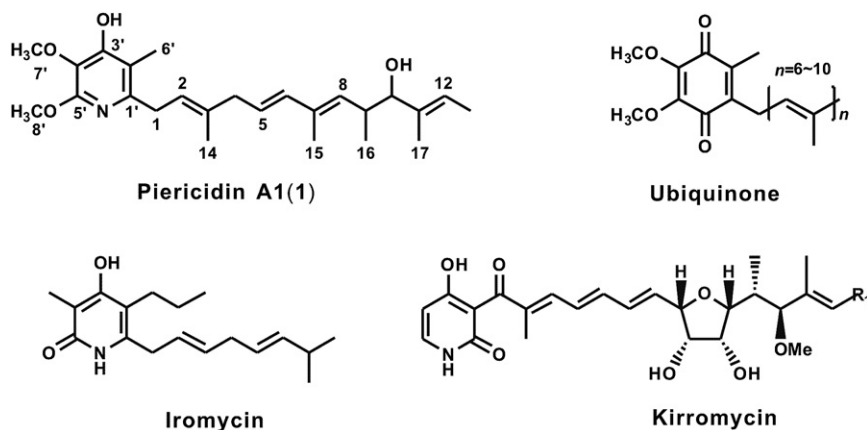


**Figure 1. Chemical Structures of  $\alpha$ -Pyridones**

See also Figure S1 and Table S1.

terminal thioesterase (TE) in hydrolyzing a  $\beta$ ,  $\delta$ -diketo thioester polyketide product has also been demonstrated. To our knowledge, this study revealed a new pathway for biosynthesis of  $\alpha$ -pyridone natural products that is different from the previously characterized  $\alpha$ -pyridone pathways.

## RESULTS

### Locating the Biosynthetic Locus of **1** in *S. piomogeeus* var. *Hangzhouwanensis*

*S. piomogeeus* var. *Hangzhouwanensis* was isolated from soil in a screening program for bioactive agents and exhibits strong antibacterial and insecticidal activity. Liquid chromatography-mass spectrometry (LC-MS) analysis of the culture revealed a peak retention time at 17.3 min with the UV spectrum and mass/charge ( $m/z$ ) signal ( $m/z$  416.5 [ $M+H$ ]<sup>+</sup>) consistent with those reported for **1**. Large-scale fermentation, extraction, and subsequent reverse-phase high-pressure liquid chromatographic (RP-HPLC) purification led to the purification of an amorphous colorless powder at the yield of 10 mg/l. After NMR analysis, including <sup>1</sup>H-NMR, <sup>13</sup>C-NMR, <sup>1</sup>H-<sup>13</sup>C-heteronuclear multiple-bond correlation (HMBC), <sup>1</sup>H-<sup>13</sup>C-heteronuclear multiple-quantum correlation (HMQC), and <sup>1</sup>H-<sup>1</sup>H correlation spectroscopy (COSY), the structure was identified as **1** (Figure 1) (Table S1 available online).

To identify genes involved in biosynthesis of **1**, we performed whole genome sequencing of *S. piomogeeus* var. *Hangzhouwanensis* on the Roche 454 sequencing platform. Approximately 20-fold coverage of sequence was generated and assembled into 917 contigs that span 9.15 Mb, which is typical of a *Streptomyces* genome (Bentley et al., 2002). Using Glimmer 3.0 and an online BLASTP program, we translated the whole genome nucleotide sequence into corresponding protein information, and found 30 contigs that contain genes encoding typical type I PKS modules. Among these, a 26 kb contig (contig A) was identified as a candidate potentially responsible for biosynthesis of **1**. Contig A encodes proteins with putative function as two complete modular PKSs (PieA5, PieA6), an amidotransferase (PieD), a hypothetical protein (PieC), two methyltransferases (PieB1 and PieB2), and a monooxygenase (PieE).

To test whether these genes are involved in the biosynthesis of **1**, a 17 kb region on contig A, which includes *pieA5*, *pieA6*, *pieB1*, *pieC*, and *pieD*, was deleted by the insertion of the apra-

mycin resistance cassette (Figure S1). As expected, the deletion mutant completely abolished production of **1**, confirming that the deleted genes are essential for the biosynthesis of **1** (Figure 2).

### Assembly of Whole Biosynthetic Gene Cluster

Previous feeding experiments and the structure of **1** suggest that a type I PKS containing nine colinear modules should be responsible for **1** biosynthesis, while only two intact PKS modules were found on contig A. To obtain the entire biosynthetic gene cluster, we screened approximately 2,304 clones of the *S. piomogeeus* var. *Hangzhouwanensis* genomic library by PCR. Eight overlapping cosmids were identified and revealed that contig A is flanked by a 21 kb contig (contig B) and a 49 kb contig (contig C). Contig B contains three type I PKS genes (*pieA2*, *pieA3*, and *pieA4*), and regulatory genes and transporters are present on contig C. Using the same strategy, contig D, a 26 kb contig with a regulatory gene (*pieR*) and a PKS gene (*pieA1*), is localized upstream of contig B. Three gaps between the four contigs were bridged by PCR. In total, the four contigs (contigs A–D) that contain the putative biosynthetic genes span ~130 kb on the chromosomal DNA of *S. piomogeeus* var. *Hangzhouwanensis*. As no apparent open reading frames (ORFs) were found in the 10 kb region immediately upstream of *pieE*, *pieE* was considered to be the upstream boundary of the *pie* gene cluster. The other boundary gene (*pieR*) was predicted by the juxtaposition of a gene encoding the membrane protein and a set of putative primary metabolic genes that lack significant similarity to those involved in secondary metabolite biosynthesis. Together, the putative cluster consists of six PKS genes, five post-PKS tailoring genes, and one regulatory gene (Figure 3; Table 1).

### Bioinformatic and Functional Analysis of the Gene Cluster

#### Genes Encoding PKSs

We identified six ORFs (*pieA1* to *pieA6*) encoding typical modular type I PKS, which consist of a loading module and eight extension modules (shown later in Figure 6). The PKSs are responsible for the formation of the polyketide backbone of **1**, by selective incorporation of one acetyl-CoA, three molecules of malonyl-CoA, and five molecules of methylmalonyl-CoA in an assembly-line fashion.

All eight ketosynthase (KS) domains except the KS in the loading module contain the conserved Cys-His-His residues as a catalytic triad. Similarly, corresponding active site motifs are also present in the AT, KR, DH, ER, and ACP domains (Figure S2), which indicate that all the PKS domains, except the KS in the loading module, are likely to be functional. Based on predictions by the PKS-NRPS software (Ansari et al., 2004), the AT domains

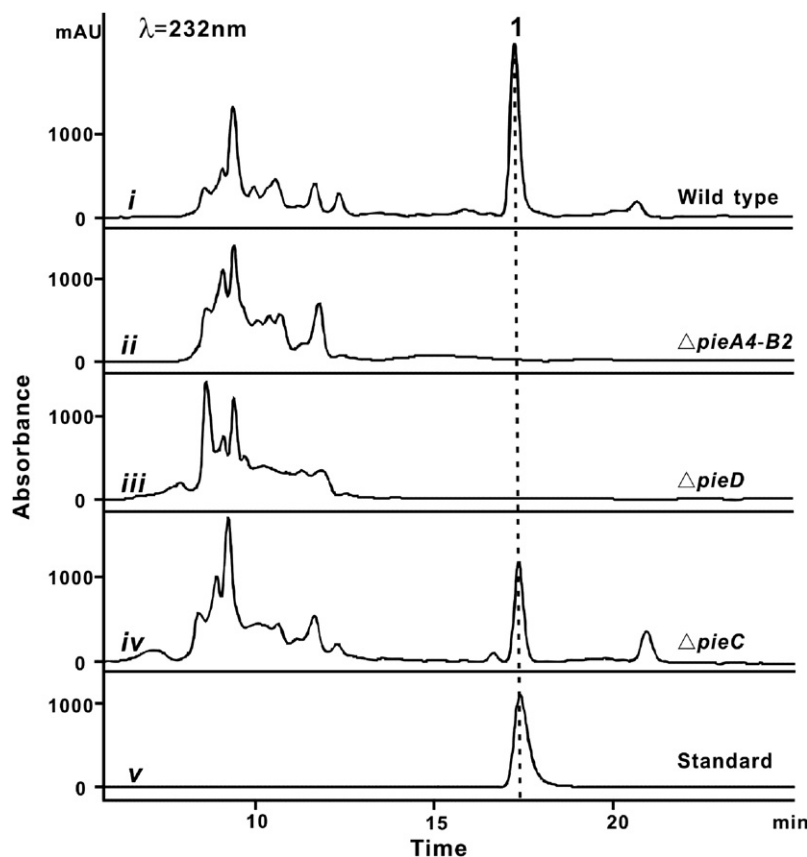


**Figure 2. LC-MS Analysis of Piericidin A1 Production in the Wild-Type and Mutant Strains of *Streptomyces piomogoeus* var. *Hangzhouwanensis***

Double crossover replacement of a 17 kb fragment (*pieA4-B2*) (trace ii), and double crossover replacement of *pieD* (trace iii) and *pieC* (trace iv); the standard was purified from the wild-type strains (trace i) and identified by NMR (trace v). The details for construction and confirmation of these mutants are described in Figure S1.

which contains the adenylation domain, is likely responsible for activation and conversion of the carboxyl group to an amide through an acyl adenylate intermediate in an ATP-dependent manner (Boehlein et al., 1998; Tesson et al., 2003). PieD is therefore predicted to catalyze the transfer of an amino group to the carboxylic acid, which is the off-loaded polyketide intermediate synthesized by PieA.

PieC is a small protein (171 aa) annotated as a hypothetical protein but belonging to the SRPBCC superfamily. This superfamily has a deep hydrophobic ligand-binding pocket and includes the polyketide cyclase TcmF2 in tetraenomycin biosynthesis (Shen and Hutchinson, 1993). Although PieC only shares 26% identity with TcmF2, we tentatively assigned PieC as the enzyme responsible for the cyclization of the  $\alpha$ -pyridone ring.

in modules 4, 6, and 8 are specific for malonyl-CoA, while the AT domains in modules 1, 2, 3, 5, and 7 are specific for methylmalonyl-CoA. This agrees with the expected elongation steps based on the colinearity rule of modular PKS and the proposed pathway of **1**.

A PKS chain-terminating TE is appended at the C terminus of module 8. The Pie TE domain shares high sequence similarity with typical type I PKS TEs, such as the TE domains of 6-deoxyerythronolide B synthase (DEBS) (39% identity) and pikromycin synthase (PICS) (39% identity). Comparison of the three TE domains indicated that they share the conserved Ser-Asp-His catalytic triad in the  $\alpha/\beta$  hydrolase family (Figure S2H).

#### Genes Involved in $\alpha$ -Pyridone Ring Formation

Two genes downstream of the PKSs, *pieC* and *pieD*, are likely involved in the formation of the  $\alpha$ -pyridone ring. PieD is a putative amidotransferase that shows high sequence identity to PcsA in rimocidin B biosynthesis (58% identity) (Seco et al., 2010), OxyD in oxytetracycline biosynthesis (53% identity) (Zhang et al., 2006), and TsrT in thiostrepton biosynthesis (51% identity) (Kelly et al., 2009). These proteins belong to the class II glutamine amidotransferases (GATs), which can transfer a nitrogen group to a carboxylic acid substrate using ammonia or glutamine as amine donors in the presence of ATP (Massière and Badet-Denisot, 1998). Similar to other characterized class II GATs, PieD consists of an N-terminal glutaminase domain and a putative C-terminal synthetase domain. The N-terminal domain containing the conserved cysteine is predicted to hydrolyze glutamine into glutamic acid and ammonia, while the C-terminal domain,

To probe the roles of *pieC* and *pieD* in the biosynthesis of **1**, we inactivated the two genes individually by replacing each gene with an apramycin resistance cassette using REDIRECT strategy (Gust et al., 2003) (Figure S1). Cultures of both mutants were extracted and analyzed by LC-MS. As shown in Figure 2, the production of **1** is completely abolished in the  $\Delta pieD$  mutant, which is in line with the putative role of PieD in the amidation and formation of the  $\alpha$ -pyridone ring. However, no polyketide shunt product, such as the expected free  $C_{18}$  linear carboxylic acid or the  $\alpha$ -pyrone, were detected in the extract either. This may be due to the instability of the  $\beta$ ,  $\delta$ -diketo carboxylic acid, which may be degraded by the fatty acid catabolic pathway in the cell. In contrast, deletion of *pieC* led to a decrease in the titer of **1** to approximately 35%–50% of wild-type levels (Figure 2). Therefore, PieC is not an essential enzyme for the biosynthesis of **1**, or its function may be complemented by other endogenous cyclases. This does not conflict with the proposed  $\alpha$ -pyridone cyclization step associated with PieC. While this cyclization can occur spontaneously after amidation of the terminal carboxylic acid (shown later in Figure 6), the presence of PieC may increase this reaction rate to promote a more efficient production of **1**.

#### Genes Involved in Modification

In addition to the polyketide assembly and pyridine ring formation, a set of postassembly modification enzymes encoded by *pieB1*, *pieB2*, and *pieE* are present in the *pie* gene cluster. PieB1 is homologous to S-adenosylmethionine (SAM)-dependent methyltransferases, such as Aurl (58% identity) in the

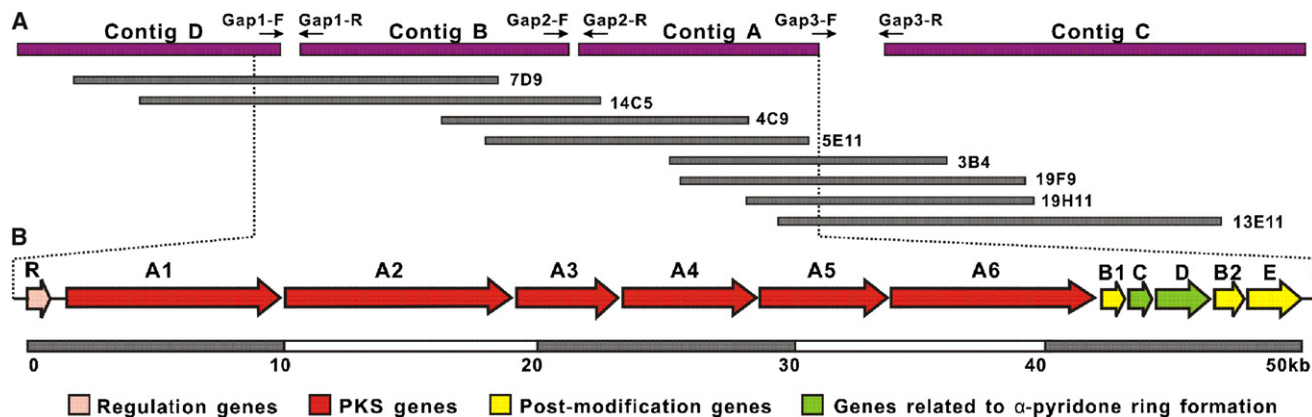


**Figure 3. Localization and Organization of the Piericidin A1 Biosynthetic Gene Cluster**

(A) Physical map of biosynthetic gene clusters. The horizontal bar indicate the involved 454 whole genome sequence contigs, the small black arrows indicate the primers for gap closure of contigs generated from 454 sequencing, and the horizontal lines indicate individual cosmids.

(B) Gene organization of the *pie* biosynthetic gene clusters. The proposed functions for the individual ORFs are summarized in Table 1.

aureothin pathway (He and Hertweck, 2003) and JerF (43% identity) in the jerangolid pathway (Julien et al., 2006). PieB2 shows high sequence similarity to the *O*-methyltransferase (50% identity) in the ubiquinone pathway (McLeod et al., 2006) and StiK (49% identity) in the stigmatellin pathway, which is also an electron transport inhibitor (Gaitatzis et al., 2002). It is interesting that methylation of the two adjacent hydroxyl groups on ubiquinone Q is catalyzed by a single *O*-methyltransferase, Coq3 (James et al., 2010), while two *O*-methyltransferases are involved in the tailoring of **1**.

PieE is a putative FAD-dependent monooxygenase and shares 50% identity to MhqA from *Bulkholderia* sp. (Tago et al., 2005) and 46% identity to TfdB isolated from a metage-

nomic screening (Lu et al., 2011), both of which are involved in hydroxylation of phenolic rings. Thus, PieE is likely responsible for the hydroxylation of the six-membered  $\alpha$ -pyridone ring.

#### Genes for Regulation and Putative Transportation

The gene *pieR* located upstream of the PKS modular assembly line belongs to the *Streptomyces* antibiotic regulatory proteins (SARPs) family (Wietzorrek and Bibb, 1997) and encodes for the pathway-specific regulatory protein in the *pie* gene cluster. Genes encoding for self-resistance were not found within the *pie* gene cluster, but five putative ABC transporters were found downstream of the PKS gene cluster separated by a 10 kb non-coding region and may function as transmembrane transporters exporting **1** out of cells. It is equally possible that the *pie* gene

**Table 1. Deduced Functions of ORFs of Piericidin A1 Biosynthetic Gene Cluster**

Protein	Amino Acids	Proposed Function	Protein Homolog and Origin	Identity/Similarity (%)	GenBank Accession Number
PieR	199	Transcriptional regulator	AurD [ <i>Streptomyces thioluteus</i> ]	53/66	CAE02599
PieA1	2,562	Modular PKS (KS <sub>A</sub> -ATa-ACP-KS-ATp-DH-KR-ACP)	ChiA1 [ <i>Streptomyces Antibioticus</i> ]	51/62	AAZ77693.1
PieA2	3,379	Modular PKS (KS-ATp-KR-ACP-KS-ATp-DH-KR-ACP)	TamAII [ <i>Streptomyces</i> sp. 307-9]	57/68	ADC79638.1
PieA3	1,724	Modular PKS (KS-ATa-DH-KR-ACP)	Baf-AS3 [ <i>Streptomyces lohii</i> ]	63/73	ADC79618.1
PieA4	2,145	Modular PKS (KS-ATp-DH-ER-KR-ACP)	Polyketide synthase [ <i>Streptomyces platensis</i> ]	59/71	BAH02268.1
PieA5	1,874	Modular PKS (KS-ATa-DH-KR-ACP)	Polyketide synthase [ <i>Streptomyces aizunensis</i> ]	57/68	AAX98191.1
PieA6	2,412	Modular PKS (KS-ATp-ACP-KS-ATa-ACP-TE)	AVES 4 [ <i>Streptomyces avermitilis</i> MA-4680]	56/67	NP_822118.1
PieB1	228	Methyltransferase	<i>O</i> -methyl transferase [ <i>Streptomyces thioluteus</i> ]	58/74	CAE02607.1
PieC	171	Hypothetical protein	Hypothetical protein RER_46650 [ <i>Rhodococcus erythropolis</i> PR4]	40/54	YR_002768112.1
PieD	587	Asparagine synthase	Asparagine synthase [ <i>Saccharopolyspora erythraea</i> NRRL 2338]	63/75	YP_001108189.1
PieB2	258	Methyltransferase	Methyltransferase [ <i>Stigmatella aurantiaca</i> ]	49/64	CAD19094.1
PieE	587	Monooxygenase, FAD-bind protein	Methylhydroquinone monooxygenase [ <i>Pseudomonas putida</i> ]	50/64	BAJ19104.1

ATp, acyl transferases specific to methylmalonyl-CoA; ATa, acyl transferases specific to malonyl-CoA.

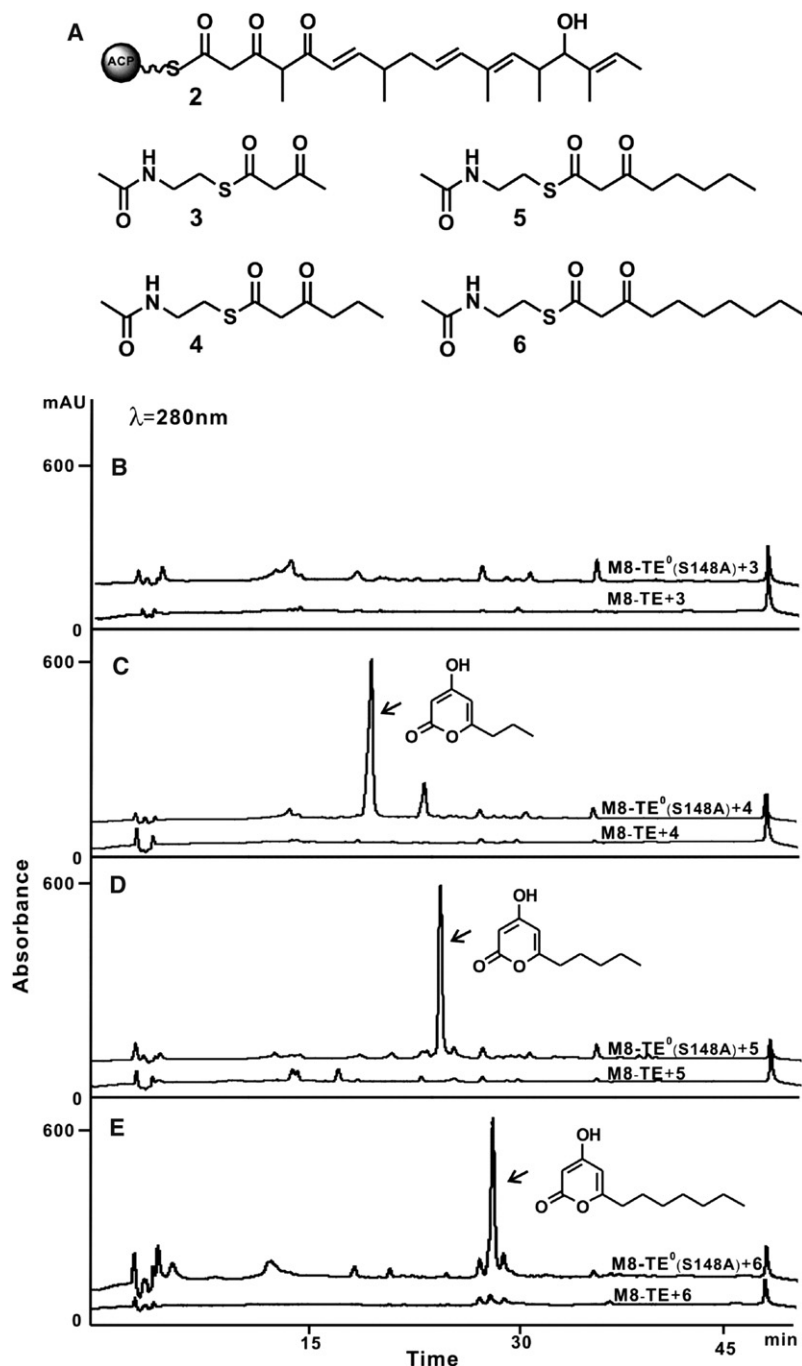


**Figure 4. In Vitro Assays of Recombinant Proteins Module 8-TE and Mutant Module 8-TE<sup>0</sup> (S148A) with  $\beta$ -Keto SNACs and Malonyl-CoA**

(A) Structures of various substrate mimics: **2** is the native substrate for Pie TE; **3** (3-oxobutanoyl-SNAC), **4** (3-oxohexanoyl-SNAC), **5** (3-oxooctanoyl-SNAC), and **6** (3-oxodecanoyl-SNAC) are the substrate mimics used in in vitro assays.

(B–E) are the HPLC profiles of the organic extract from reactions incubating enzymes with malonyl-CoA and substrates **3** (B), **4** (C), **5** (D), and **6** (E).  $\alpha$ -Pyrone products were clearly detected in assays using substrate **4** (C), **5** (D), and **6** (E) during incubation with mutant module 8-TE<sup>0</sup> (S148A) and malonyl-CoA. The three different  $\alpha$ -pyrone products were determined by MS and UV absorption shown in Figure S5, as well as one synthesized standard. See also Figures S3, S4, and S6.

ketide product is catalyzed by a terminal TE domain via intramolecular nucleophilic attack of an internal nucleophile on the thioester carbonyl to generate macrocyclic compounds. Compared to the well-known macrocyclic polyketide pathways, modular type I PKSs involved pathways utilize the C-terminal TE domains to catalyze hydrolytic release of polyketide product are less common. The SpiJ-TE in the spirangien biosynthesis (Frank et al., 2007) and the TMC-TE in the tautomycin gene cluster (Li et al., 2009; Scaglione et al., 2010) are two of the few examples. Given that Pie TE contains the highly conserved GxSxG and Ser-His-Asp catalytic triad that are characteristic of  $\alpha/\beta$  hydrolase family of serine hydrolases, it is likely that Pie TE is responsible for the hydrolytic step.

To gain insights into this crucial step in the  $\alpha$ -pyridone ring formation, we attempted to reconstitute the function of the last module appended with the terminal TE (module 8-TE) in vitro. The natural substrate of module 8-TE is the  $\beta$ -ketoacyl thioester polyketide intermediate synthesized by the upstream modules 1–7. Module 8 is expected to catalyze one round of chain elongation with one malonyl extender unit to yield the  $\beta$ ,  $\delta$ -diketoacyl-S-ACP (**2**). To probe the function of module 8-TE, various linear  $\beta$ -ketoacyl-S-N-acetylcysteamine (SNAC)

thioesters, including 3-oxo-butanoyl-SNAC (**3**), 3-oxo-hexanoyl-SNAC (**4**), 3-oxo-octanoyl-SNAC (**5**), and 3-oxo-decanoyl-SNAC (**6**) (Oikawa et al., 1978) (Figure 4A) were synthesized to mimic the upstream polyketide intermediate. Normally, in the absence of a hydrolytic TE domain, one would expect the  $\beta$ ,  $\delta$ -diketo thioester to undergo spontaneous enolization and cyclization to form the  $\alpha$ -pyrone. In the presence of a hydrolytic TE, such as the one proposed here, the corresponding  $\beta$ ,  $\delta$ -diketo acid is expected to be released. Comparing the results of the precursor feeding assay with those using module 8-TE<sup>0</sup> (in which the TE active site serine in the Ser-His-Asp catalytic triad is

#### In Vitro Enzymatic Assay of Module 8-TE and Mutant Module 8-TE<sup>0</sup> (S148A)

Based on the catalytic role of PieD proposed earlier, we hypothesized that the terminal TE domain in the *pie* PKS should hydrolyze the polyketide chain into the linear  $\beta$ ,  $\delta$ -diketo carboxylic acid, which serves as the substrate for PieD. Typically in bacterial type I polyketide biosynthesis, the off-loading of poly-

ketide product is catalyzed by a terminal TE domain via intramolecular nucleophilic attack of an internal nucleophile on the thioester carbonyl to generate macrocyclic compounds. Compared to the well-known macrocyclic polyketide pathways, modular type I PKSs involved pathways utilize the C-terminal TE domains to catalyze hydrolytic release of polyketide product are less common. The SpiJ-TE in the spirangien biosynthesis (Frank et al., 2007) and the TMC-TE in the tautomycin gene cluster (Li et al., 2009; Scaglione et al., 2010) are two of the few examples. Given that Pie TE contains the highly conserved GxSxG and Ser-His-Asp catalytic triad that are characteristic of  $\alpha/\beta$  hydrolase family of serine hydrolases, it is likely that Pie TE is responsible for the hydrolytic step.

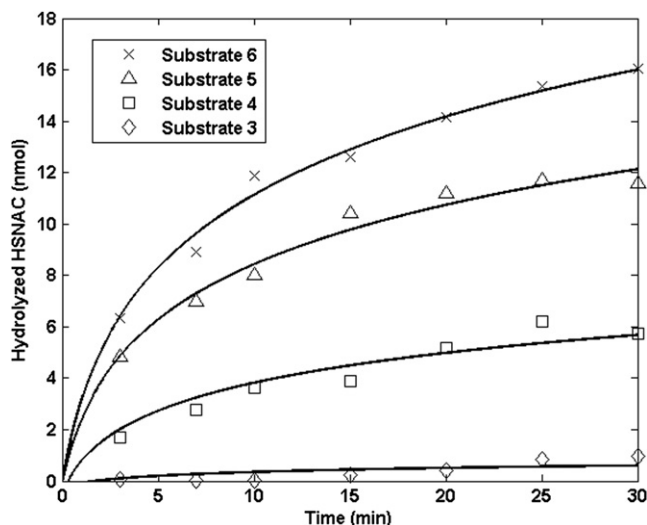


**Figure 5. Kinetic Analysis of Various Substrate Mimics**

Detection of the hydrolysis activity of TE domain in recombinant module 8-TE by Ellman's reagents with substrate mimics **3**, **4**, **5**, and **6**. The concentration of hydrolyzed free SNAC on the y axis was based on absorbance values that have been corrected for the background rate of hydrolysis by mutant module 8-TE<sup>0</sup> (S148A) and in the absence of enzyme to obtain the net hydrolysis rate for Pie TE domain. See also Figures S5, S6, and S7.

mutated to alanine S148A) will provide useful insights into the fate of the  $\beta$ ,  $\delta$ -diketoacyl thioesters product.

To clone the stand-alone module 8-TE, we first predicted the intermodule boundary using PKS online software (Ansari et al., 2004) and amino acid sequence alignment. The *holo* form of module 8-TE and module 8-TE<sup>0</sup> (S148A) with a 20 amino acid linker at the N terminus were then cloned and solubly expressed in *Escherichia coli* BAP1 (Pfeifer et al., 2001). The purity and size (147 kDa) of the recombinant proteins were determined by SDS-PAGE, shown in Figure S3.

On incubation of module 8-TE with malonyl-CoA and SNAC substrates **3**, **4**, or **5** followed by extraction and product analysis, no clear chain-extended product such as the linear  $\beta$ ,  $\delta$ -diketo carboxylic acid can be detected by LC-MS (Figure 4). However, when substrate **6** was supplemented to the reaction mixture, we were able to detect a small peak with  $[M + H]^+ m/z$  of 185 (data not shown). Although the structure of the corresponding compound cannot be verified,  $m/z$  and retention time suggests that it may be undecane-2,4-dione, which is the decarboxylated product of  $\beta$ ,  $\delta$ -diketo carboxylic acid. In the absence of either malonyl-CoA or module 8-TE, the peak is not detected. In addition, to detect the presence of linear  $\beta$ ,  $\delta$ -diketo carboxylic acid that may have been hydrolyzed by the TE domain, we attempted to use the fluorophore fluoresceinamine as a conjugation reagent that can react with 1-ethyl-3-(3-dimethylaminopropyl) carbodiimide (EDC)-activated carboxylic acid. Subsequent to incubation of module 8-TE with **6**, the reaction mixture were extracted with ethyl acetate and the organic phase was dried. Upon reacting with EDC and fluoresceinamine, LC-MS analysis revealed a peak with a UV spectrum consistent with the fluorophore group and a  $[M + H]^+ m/z$  of 558, which corresponds to the calculated molecular weight for fluoresceinamine-conjugated **3**, 5-dioxo-

decanoic acid (Figure S4). This peak cannot be found in the absence of any reaction component, or when module 8-TE is substituted with module 8-TE<sup>0</sup> (S148A) (Figure S4). Consistent with the detection of the putative undecane-2,4-dione, assays with shorter  $\beta$ -ketoacyl thioesters (**3**, **4**, or **5**) did not afford any fluoresceinamine-labeled compounds, indicating that the longer substrate may be preferred by TE domain. The observed low amount of the hydrolyzed linear polyketide product in wild-type module 8-TE assays is likely due to rapid degradation of the unstable  $\beta$ ,  $\delta$ -diketo carboxylic acid products.

In contrast to module 8-TE, in vitro assays of the mutant module 8-TE<sup>0</sup> (S148A) with malonyl-CoA and **4**, **5**, or **6** resulted in production of different polyketide products (Figures 4C–4E), while no obvious product can be detected for **3**. All these enzymatic products synthesized from **4**, **5**, and **6** exhibit characteristic UV spectra and  $m/z$  values that match the predicted triketide  $\alpha$ -pyrone products (Figures S5B–S5D). To verify that these pyrone products are indeed resulted from a single round of extension catalyzed by PKS module 8, we assayed module 8-TE<sup>0</sup> (S148A) with 2- $[^{13}C]$ -malonyl-CoA and SNAC substrates. As expected, LC-MS analysis showed that the  $m/z$  values of all three pyrone products from **4**, **5**, and **6** were increased by 1 Da as a result of incorporating one molecular 2- $[^{13}C]$ -malonyl-CoA (Figure S6). Further confirmation was obtained by the chemical synthesis of 4-hydroxy-6-propyl-2H-pyran-2-one as a standard; the UV spectra, retention time, and mass spectra of the standard matches the corresponding enzymatic product produced by module 8-TE<sup>0</sup> (S148A) from substrate **4** (Figure S5A). These pyrone shunt products can also be detected in trace amount in in vitro assays with wild-type module 8-TE, but only at 1%–3% of the amount obtained with mutant module 8-TE<sup>0</sup> (S148A) (Figure S7). Taken together, the postulated function of Pie TE as a hydrolytic thioesterase is strongly supported, and Pie TE is suggested to hydrolyze the polyketide product from module 8 ACP to prevent  $\alpha$ -pyrone shunt product formation.

In a previous study, the hydrolysis activity of DEBS TE was determined by detection of free sulfhydryl group by Ellman's reagent (5,5'-dithio-2-nitrobenzoic acid) (Lu et al., 2002). Using the same method, we detected hydrolysis of **3**, **4**, **5** and **6** by module 8-TE by measuring the increment of absorbance at 412 nm. The time course of the hydrolysis assays was measured over a 30 min reaction period as shown in Figure 5. Different controls were made to eliminate the effects of various backgrounds. The slight increment detected in the control with mutant module 8-TE<sup>0</sup> (S148A) could be due to the single turn-over loading of the acyl-SNAC substrate onto the KS domain, which released low amount of SNAC as free thiols (data not shown). The increased absorbance at 412 nm over time can be clearly detected against the background for all the tested substrates except the diketide SNAC. This showed that Pie TE also exhibits a higher preference for longer chain substrates, with the longest C10 substrate being hydrolyzed at the fastest reaction rate.

## DISCUSSION

In this study, we identified the biosynthetic gene cluster of the mitochondrial complex I inhibitor **1** from the producer strain *S. piomogeues* var. Hangzhouwanensis by genome scanning.

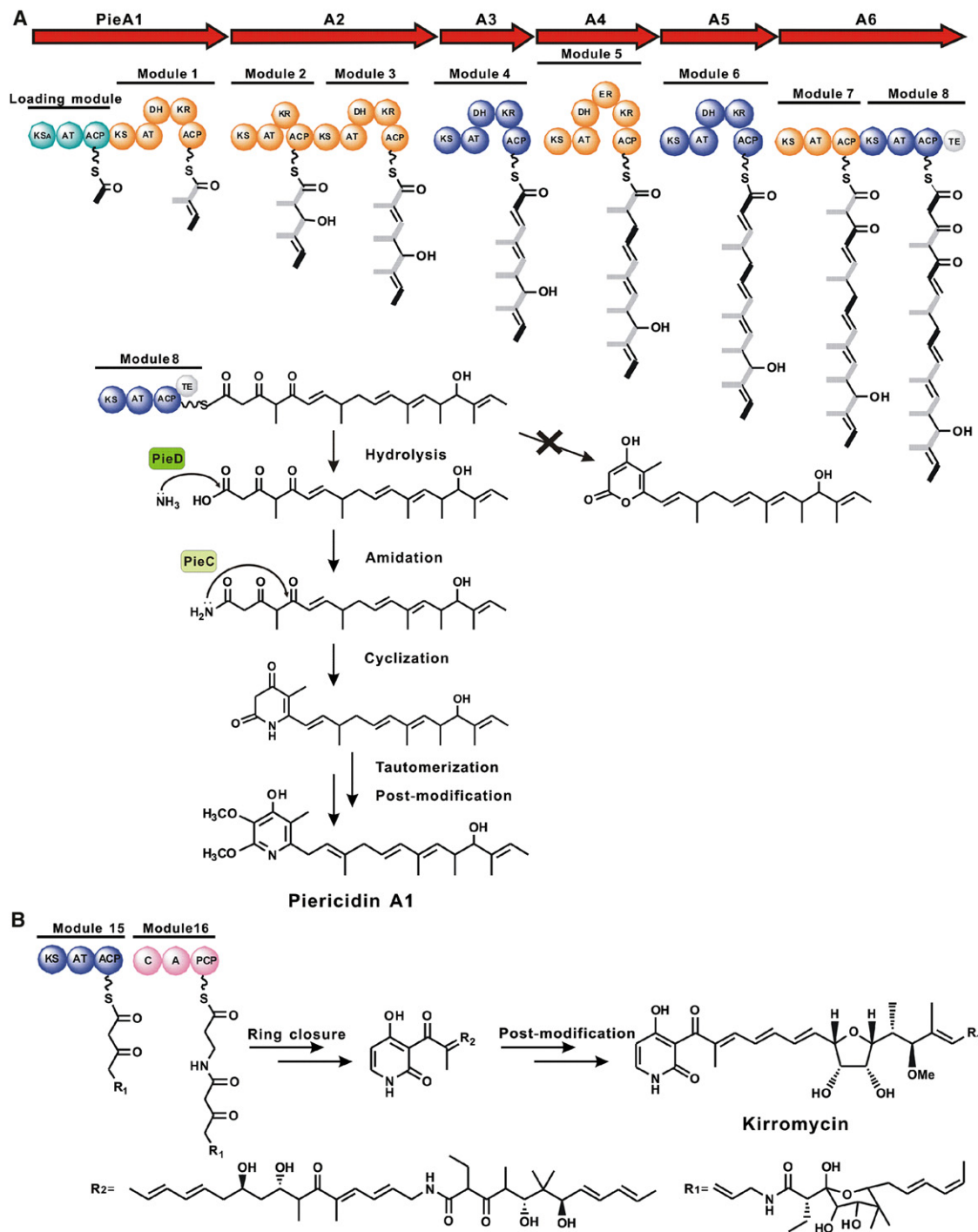


**Figure 6. Proposed Biosynthetic Pathway of Piericidin A1**

(A) Proposed biosynthetic pathway of **1**. PKS extending modules specific to methylmalonyl-CoA units are shaded in orange, and those specific to malonyl-CoA are shaded in blue; the loading module is shaded in turquoise.

(B) Proposed pathway for  $\alpha$ -pyridone ring formation in antibiotic kirromycin biosynthesis. The  $\beta$ -alanine is added to the polyketide chain by a NRPS module, followed by an intramolecular cyclization to form the  $\alpha$ -pyridone ring. See also Figure S2.

According to the *in vivo* targeted gene inactivation study and *in vitro* biochemical characterization of Pie module 8, the proposed biosynthetic pathway for **1** is outlined in Figure 6. The *pieA1*-*pieA6* encode for a type I PKS harboring one loading

module and eight extension modules to afford the polyketide backbone and form the  $\alpha$ -pyridone ring.

The presence of PieD, an ATP-dependent class II GAT, in the *pie* gene cluster suggests that the formation of the  $\alpha$ -pyridone

ring may involve initial hydrolysis of the linear unsaturated polyketide chain, followed by amidation of the carboxylic acid intermediate by PieD. PieD shows high sequence homology to amidotransferases in secondary metabolic pathways, such as OxyD and FdmV. For OxyD in the oxytetracycline gene cluster, it proved to be essential for amidation of the malonamate starter unit at the terminal carboxylic acid of malonyl-CoA or malonyl-ACP (Zhang et al., 2006). Another representative enzyme, FdmV, can catalyze similar amidation reaction in fredericamycin biosynthesis (Wendt-Pienkowski et al., 2005). When FdmV was inactivated, the mutant accumulated the carboxylic acid shunt product but not the corresponding amide. FdmV was also shown to convert the corresponding carboxylic acid to amide product in vitro (Chen et al., 2010). Therefore, PieD is likely to catalyze the amidation of the terminal carboxylic group of the linear polyketide intermediate hydrolyzed by the TE domain. This mechanism is supported by a previous feeding study on iromycin (Figure 1), which shares an  $\alpha$ -pyridone ring with **1**. The successful incorporation of  $(^{15}\text{NH}_4)_2\text{SO}_4$  into iromycin (Surup et al., 2007), agrees with the involvement of an amidation step in the  $\alpha$ -pyridone ring formation, as this family of amidotransferases can utilize ammonia as an amino donor.

Accordingly, inactivation of the *pieD* should yield the linear carboxylic acid released by the TE domain; however, such intermediate cannot be detected because of the instability of the compound. To better understand the mechanism of the  $\alpha$ -pyridone formation, we turned to characterize the terminal PKS-releasing module in vitro. In the in vitro assays with module 8 appended with mutated TE<sup>0</sup> (S148A), we can observe the formation of pyrone products, which are synthesized from the supplied  $\beta$ -ketoacyl thioesters substrates after one round of decarboxylative chain extension and spontaneous lactonization of the  $\beta$ ,  $\delta$ -diketo thioester. In contrast, the production of  $\alpha$ -pyrone products are nearly abolished in assays with module 8 appended with wild-type TE domain. Therefore, the TE domain essentially prevents the formation of pyrones as shunt products by efficiently hydrolyzing the  $\beta$ ,  $\delta$ -diketo thioester from the PieA. In contrast to DEBS TE, which can hydrolyze the non-native diketo-SNAC (Lu et al., 2002), only longer chain SNAC substrates (C6–C10) can be hydrolyzed as detected by the Ellman assays. Compared to C-terminal PKS TEs that catalyze macrolactonization, such as the well-characterized DEBS and Pik TEs, hydrolytic PKS TE domains are relatively rare. In the previous study on Pik TE, a “hydrophilic barrier” at Gln183, Ala127, and C5-hydroxyl group of the pentaketide are proved to be a key factor which can drive the acyl polyketide chain back into the TE substrate channel to allow macrolactone formation (Akey et al., 2006). In contrast, the side chain Gln183 in this region is replaced by hydrophobic Leu107 in Pie TE, and this may cause the corresponding hydrophilic barrier region in Pie TE to be less functional. Recently, the structure of the hydrolytic TE domain in the tautomycin biosynthesis has been solved (Scaglione et al., 2010). This TMC TE (38% sequence similarity with Pie TE) mediates the direct hydrolysis rather than intermolecular cyclization. The His138 can also be found in TMC TE (corresponding to Leu107 in Pie TE and to Gln183 in Pik TE and DEBS TE). It was proposed that the functional difference between the macrolactone-forming TE and the hydrolytic TE is due to the relatively constrained substrate

chamber (Scaglione et al., 2010), and may be the same case in Pie TE.

Although amidation of the carboxylic acid by PieD is not proven in vitro because of the inability to obtain soluble PieD by heterologous expression in either *E. coli* or *S. lividans* K4, the hydrolytic role of Pie TE and the homology of PieD to class II GATs indicate that the carboxylic acid is likely to be the substrate for PieD. Upon amidation of the linear  $\beta$ ,  $\delta$ -diketo carboxylic acid by PieD, PieC was proposed to mediate the cyclization of the corresponding amide to form the  $\alpha$ -pyridone ring. PieC belongs to a family of enzymes that includes type II polyketide cyclases. For example, one of the well-characterized cyclases is TcmF2 (26% identity to PieC), which was characterized to be responsible for the polyketide cyclization via an intramolecular aldol condensation in an in vitro experiment (Shen and Hutchinson, 1993; Thompson et al., 2004). So far, such cyclases are rarely involved in the type I PKS pathway. It is interesting that inactivation of the *pieC* gene led to significant reduction of **1** production but not complete loss of production. This suggests that *pieC* may participate in the  $\alpha$ -pyridone ring cyclization but that the  $\alpha$ -pyridone ring is likely to form spontaneously without PieC, albeit at lower efficiency. This is similar to the biosynthesis of some type II polyketide antibiotics, where the ring closure can be enzymatic catalyzed by cyclases or via spontaneous, nonregioselective condensation (Kendrew et al., 1999; Zhang and Tang, 2009). Subsequent tailoring modifications of the  $\alpha$ -pyridone ring with one hydroxylation and two *O*-methylations yield **1**.

The mechanism proposed in this study for the  $\alpha$ -pyridone ring formation is in stark contrast to the biosynthesis of other known  $\alpha$ -pyridone-ring-containing antibiotics that involve hybrid PKS-NRPS systems. In biosynthesis of kirromycin, the nitrogen atom on the  $\alpha$ -pyridone ring originates from  $\beta$ -alanine. The  $\beta$ -alanine precursor is synthesized from decarboxylation of aspartate and introduced to the polyketide chain by the terminal NRPS module at the end of the PKS-NRPS assembly line followed by an intramolecular cyclization (Figure 6) (Weber et al., 2008). Fungal  $\alpha$ -pyridone compounds, such as tenellin and aspyridone, are produced by iterative PKS-NRPS hybrid systems and also incorporate an amino acid into the polyketide chain. The direct product of the PKS-NRPS is a five-membered tetramic acid (Xu et al., 2010), and a P450 oxidase is required to convert the tetramic acid moiety to an  $\alpha$ -pyridone via a unique oxidative ring expansion (Halo et al., 2008). Unlike these hybrid PKS-NRPS systems, no amino acid is incorporated into the polyketide chain of **1**, and the involvement of a highly reactive  $\beta$ ,  $\delta$ -diketo thioester intermediate synthesized by the Pie PKS requires that the C-terminal fused TE domain work efficiently for linear polyketide chain hydrolyzed in concert with the subsequent amidation and cyclization steps to afford the final  $\alpha$ -pyridone ring.

## SIGNIFICANCE

**The pyridone class of antibiotics exhibits promising bioactivities, including antimicrobial, antifungal, and antitumor. In this study, we have identified the gene cluster of **1** and revealed a novel pathway for biosynthesis of  $\alpha$ -pyridone system that is strikingly different from the previously characterized hybrid polyketide synthase-nonribosomal peptide synthetase (PKS-NRPS) involved  $\alpha$ -pyridone pathways.**

**Bioinformatic analysis, gene deletions, and in vitro biochemical characterization of the terminal Pie module 8 appended with thioesterase (TE) have shed light into the mechanism for the  $\alpha$ -pyridone ring formation in 1, which involves an unusual polyketide chain hydrolysis to linear  $\beta$ ,  $\delta$ -diketo carboxylic acid by the C-terminal TE, and an amidation by an amidotransferase PieD. This new pathway for  $\alpha$ -pyridone biosynthesis should prove general to the biosynthesis of similar  $\alpha$ -pyridone antibiotics, such as irromycin. The uncovered gene cluster information also provided a foundation for genome mining of new  $\alpha$ -pyridone antibiotics and generation of novel analogs by molecular engineering.**

## EXPERIMENTAL PROCEDURES

### Bacterial Strains and Culturing Conditions

Bacterial strains used in this study are listed in Table S2.

*S. piomogues* var. Hangzhouwanensis, the producing strain of 1, was used for piericidin A1 isolation as well as generation of mutant by REDIRECT strategy. YMS solid medium and tryptic soy broth liquid medium were used to cultivate *S. piomogues* var. Hangzhouwanensis as well as mutants. Fermentation for 1 production was performed in the liquid medium containing corn powder (35 g/l), soy powder (15 g/l), KNO<sub>3</sub> (6 g/l), MgSO<sub>4</sub> (0.5 g/l), FeSO<sub>4</sub> (0.01 g/l), (NH<sub>4</sub>)<sub>2</sub>SO<sub>4</sub> (1 g/l), and CaCO<sub>3</sub> (5 g/l), initial pH at 7.2.

*E. coli* DH10B was used for the DNA manipulation. *E. coli* ET12567 carrying pUZ8002 was used for intergeneric conjugation (Paget et al., 1999). *E. coli* BW25113 carrying plJ790 was used for REDIRECT strategy (Gust et al., 2003). *E. coli* BAP1 was used for protein expression and obtained from Professor Chaitan Khosla (Pfeifer et al., 2001).

### Plasmid and General Techniques for DNA Manipulation

Plasmids used in this study are listed in Table S2. pOJ446 was used for constructing the genomic library, pJTU1278 derived from pHZ1358 was used for gene replacement (He et al., 2010), and pMD18-T (TaKaRa) and pBlueScript II SK plus (Stratagene) were used for sequencing of DNA fragments. General procedures for *E. coli* or *Streptomyces* manipulation were carried out according to Sambrook and Russel (2001) and (Kieser et al., 2000). For selection of *streptomyces* transformants, apramycin and thiostrepton were used at concentrations of 15  $\mu$ g/ml and 12.5  $\mu$ g/ml, respectively.

### Genome Scanning and In Silico Analysis

The genomic scanning project was performed at Roche, Ltd. (Roche, Indianapolis, IN, USA). The sequencing contigs were assembled together then translated to amino acid sequence using Glimmer. ORFs were predicted with FramePlot 4.0 (<http://nocardia.nih.gov/jp4/>). We performed DNA and deduced protein sequence homology searches using BLAST (<http://blast.ncbi.nlm.nih.gov/Blast.cgi>). The prediction of PKS region was performed with the online application NRPS-PKS (<http://www.nii.res.in/nrps-pks.html>) (Ansari et al., 2004). Multiple sequence alignment was performed with CLUSTALW.

### Hydrolytic Activity Assay with SNAC Substrate

To detect the hydrolysis product of module 8-TE and mutant module 8-TE<sup>0</sup> (S148A), the in vitro assay was set up and detected as following. The reactions were performed at 100  $\mu$ l scale in 50 mM phosphate buffer (pH 8.0) in the presence of 1 mM SNAC substrate, 2 mM malonyl-CoA (or 2-[<sup>13</sup>C]-malonyl-CoA), and 10  $\mu$ M module 8-TE or mutant module 8-TE<sup>0</sup> (S148A). The reaction mixture was incubated at 30°C overnight and then terminated and extracted with 1 ml ethylacetate (EA). The organic phase was separated, evaporated to dryness, redissolved in 20  $\mu$ l of methanol, and analyzed with LC-MS analysis.

To detect the product of carboxylic acid group with fluoresceinamine, we set up the in vitro reaction as follows. The reactions were scaled up to 500  $\mu$ l and incubated at 30°C overnight; they were then terminated and extracted with 1 ml EA. The organic phase was separated, evaporated to dryness, and redissolved in 200  $\mu$ l dichloromethane. On addition of 2 mM fluoresceinamine and 3 mM 1-ethyl-3-(3-dimethylaminopropyl) carbodiimide (EDC), the reaction is

initiated and the mixture was stirred at 4°C for 4 hr. All the procedures that involve fluoresceinamine were performed in dark. For sample analysis, the reaction mixture was first washed with 800  $\mu$ l water to remove the byproducts, and the organic fraction was dried and redissolved in 30  $\mu$ l methanol before the LC-MS analysis.

For detection of the free sulfhydryl group release, Ellman's reagent assay was applied and the reaction was monitored by measuring the absorbance at 412 nm. The reactions were performed at 100  $\mu$ l scale in 50 mM phosphate buffer (pH 8.0) in the presence of 1 mM SNAC substrate, 10  $\mu$ M protein. The reaction mixture was incubated at 30°C. At 3 min, 7 min, 10 min, 15 min, 20 min, and 30 min after the reaction is initiated, 80  $\mu$ l of the reaction mixture were withdrawn and the reaction was quenched upon the addition of 20  $\mu$ l of 1M HCl. The protein was removed with a 10,000 Micropure-EZ (Amicon) ultra-filtration unit. The amount of released free sulfhydryl group was detected by mixing with 100  $\mu$ l of a saturated solution of DNTB in 50 mM phosphate buffer (pH 8.0) and 800  $\mu$ l of 50 mM phosphate buffer (pH 8.0). Several parallel control reactions were performed for each substrate. Reactions were as follows: (1) enzyme module 8-TE, SNAC, and DTNB; (2) enzyme mutant module 8-TE<sup>0</sup> (S148A), SNAC, and DTNB; (3) enzyme module 8-TE, and DTNB without SNAC; (4) enzyme mutant module 8-TE<sup>0</sup> (S148A), and DTNB without SNAC; (5) substrate and DTNB without enzyme; and (6) only DTNB.

### Synthesis of 4-6

Preparations of 3-oxoacyl-SNACs 4-6 all follow similar procedures. The synthesis of 6 is described here in detail. Octanoyl chloride was synthesized from octanoic acid and thionyl-chloride. The resulting octanoyl chloride was treated with Meldrum's acid according to general procedures in literature to synthesize octanoyl Meldrum's acid (Oikawa et al., 1978). A solution of N-acetylcysteamine (0.119 g, 1.0 mmol) in toluene (5 ml) was added to a solution of octanoyl Meldrum's acid (0.270 g, 1.0 mmol) in toluene (5 ml) in a round-bottom flask equipped with a magnetic stir bar. The reaction mixture was then stirred at 80°C for 3 hr. The solvent was removed in vacuo, and the crude product was purified by silica column chromatography (EtOAc) and then recrystallized from EtOAc to afford the 3-oxodecanoyl-SNAC as a colorless crystalline solid (0.121 g, 42%). The compound shows as a mixture of keto (major) and enol (minor) tautomers (2:1) in CDCl<sub>3</sub>. keto form: <sup>1</sup>H NMR (500 MHz, CDCl<sub>3</sub>):  $\delta$  = 0.89 (t, 3H, J = 6.9Hz, CH<sub>2</sub>CH<sub>3</sub>), 1.2-1.3 (m, 8H, Me(CH<sub>2</sub>)<sub>4</sub>), 1.58 (m, 2H, Me(CH<sub>2</sub>)<sub>4</sub>CH<sub>2</sub>), 1.97 (s, 3H, COCH<sub>3</sub>), 2.51 (t, 2H, J = 7.3Hz, Me(CH<sub>2</sub>)<sub>5</sub>CH<sub>2</sub>CO), 3.09 (m, 2H, CH<sub>2</sub>S), 3.45 (m, 2H, CH<sub>2</sub>N), 3.68 (s, 2H, COCH<sub>2</sub>CO); <sup>13</sup>C NMR (125 MHz, CDCl<sub>3</sub>):  $\delta$  = 14.2 (CH<sub>3</sub>CH<sub>2</sub>), 22.7 (CH<sub>3</sub>CO), 23.2 (CH<sub>3</sub>CH<sub>2</sub>), 23.3 (CH<sub>2</sub>CH<sub>2</sub>CO), 26.4 (CH<sub>2</sub>), 27.8 (CH<sub>2</sub>), 29.0 (CH<sub>2</sub>), 32.0 (EtCH<sub>2</sub>), 39.9 (CH<sub>2</sub>NH), 43.6 (CH<sub>2</sub>CH<sub>2</sub>CO), 57.3 (COCH<sub>2</sub>CO), 170.3 (CH<sub>3</sub>CO), 194.6 (CH<sub>2</sub>COS), 202.4 (CH<sub>2</sub>COCH<sub>2</sub>).

### ACCESSION NUMBERS

Sequencing data are accessible at GenBank under accession number HQ840721.

### SUPPLEMENTAL INFORMATION

Supplemental Information includes three tables and seven figures, and Supplemental Experimental Procedures and can be found with this article online at [doi:10.1016/j.chembiol.2011.12.018](https://doi.org/10.1016/j.chembiol.2011.12.018).

### ACKNOWLEDGMENTS

This work was supported by grants from the National Science Foundation of China, the Ministry of Science and Technology (973 and 863 Programs), China Ocean Mineral Resources R & D Association, and the Shanghai Municipal Council of Science and Technology. Work at the University of California, Los Angeles, is supported by the Camille and Henry Dreyfus Foundation.

Received: July 20, 2011

Revised: November 25, 2011

Accepted: December 22, 2011

Published: February 23, 2012

## REFERENCES

- Akey, D.L., Kittendorf, J.D., Giraldes, J.W., Fecik, R.A., Sherman, D.H., and Smith, J.L. (2006). Structural basis for macrolactonization by the pikromycin thioesterase. *Nat. Chem. Biol.* **2**, 537–542.
- Ansari, M.Z., Yadav, G., Gokhale, R.S., and Mohanty, D. (2004). NRPS-PKS: a knowledge-based resource for analysis of NRPS/PKS megasynthases. *Nucleic Acids Res.* **32** (Web Server issue), W405–W413.
- Bentley, S.D., Chater, K.F., Cerdeño-Tárraga, A.M., Challis, G.L., Thomson, N.R., James, K.D., Harris, D.E., Quail, M.A., Kieser, H., Harper, D., et al. (2002). Complete genome sequence of the model actinomycete *Streptomyces coelicolor* A3(2). *Nature* **417**, 141–147.
- Bergmann, S., Schümann, J., Scherlach, K., Lange, C., Brakhage, A.A., and Hertweck, C. (2007). Genomics-driven discovery of PKS-NRPS hybrid metabolites from *Aspergillus nidulans*. *Nat. Chem. Biol.* **3**, 213–217.
- Boehlein, S.K., Stewart, J.D., Walworth, E.S., Thirumoorthy, R., Richards, N.G., and Schuster, S.M. (1998). Kinetic mechanism of *Escherichia coli* asparagine synthetase B. *Biochemistry* **37**, 13230–13238.
- Chen, Y., Wendt-Pienkowski, E., Ju, J., Lin, S., Rajski, S.R., and Shen, B. (2010). Characterization of FdmV as an amide synthetase for fredericamycin A biosynthesis in *Streptomyces griseus* ATCC 43944. *J. Biol. Chem.* **285**, 38853–38860.
- Eley, K.L., Halo, L.M., Song, Z.S., Powles, H., Cox, R.J., Bailey, A.M., Lazarus, C.M., and Simpson, T.J. (2007). Biosynthesis of the 2-pyridone tenellin in the insect pathogenic fungus *Beauveria bassiana*. *ChemBioChem* **8**, 289–297.
- Frank, B., Knauber, J., Steinmetz, H., Scharfe, M., Blöcker, H., Beyer, S., and Müller, R. (2007). Spiroketal polyketide formation in *Sorangium*: identification and analysis of the biosynthetic gene cluster for the highly cytotoxic spirangienes. *Chem. Biol.* **14**, 221–233.
- Gaitatzis, N., Silakowski, B., Kunze, B., Nordsiek, G., Blöcker, H., Höfle, G., and Müller, R. (2002). The biosynthesis of the aromatic myxobacterial electron transport inhibitor stigmatellin is directed by a novel type of modular polyketide synthase. *J. Biol. Chem.* **277**, 13082–13090.
- Gust, B., Challis, G.L., Fowler, K., Kieser, T., and Chater, K.F. (2003). PCR-targeted *Streptomyces* gene replacement identifies a protein domain needed for biosynthesis of the sesquiterpene soil odor geosmin. *Proc. Natl. Acad. Sci. USA* **100**, 1541–1546.
- Gutman, M., Singer, T.P., Beinert, H., and Casida, J.E. (1970). Reaction sites of rotenone, piericidin A, and amytal in relation to the nonheme iron components of NADH dehydrogenase. *Proc. Natl. Acad. Sci. USA* **65**, 763–770.
- Hall, C., Wu, M., Crane, F.L., Takahashi, H., Tamura, S., and Folkers, K. (1966). Piericidin A: a new inhibitor of mitochondrial electron transport. *Biochem. Biophys. Res. Commun.* **25**, 373–377.
- Halo, L.M., Heneghan, M.N., Yakasai, A.A., Song, Z., Williams, K., Bailey, A.M., Cox, R.J., Lazarus, C.M., and Simpson, T.J. (2008). Late stage oxidations during the biosynthesis of the 2-pyridone tenellin in the entomopathogenic fungus *Beauveria bassiana*. *J. Am. Chem. Soc.* **130**, 17988–17996.
- He, J., and Hertweck, C. (2003). Iteration as programmed event during polyketide assembly; molecular analysis of the aureothin biosynthesis gene cluster. *Chem. Biol.* **10**, 1225–1232.
- He, Y., Wang, Z., Bai, L., Liang, J., Zhou, X., and Deng, Z. (2010). Two pHZ1358-derivative vectors for efficient gene knockout in *streptomyces*. *J. Microbiol. Biotechnol.* **20**, 678–682.
- Hwang, J.H., Kim, J.Y., Cha, M.R., Ryoo, I.J., Choo, S.J., Cho, S.M., Tsukumo, Y., Tomida, A., Shin-Ya, K., Hwang, Y.I., et al. (2008). Etoposide-resistant HT-29 human colon carcinoma cells during glucose deprivation are sensitive to piericidin A, a GRP78 down-regulator. *J. Cell. Physiol.* **215**, 243–250.
- James, A.M., Cochemé, H.M., Murai, M., Miyoshi, H., and Murphy, M.P. (2010). Complementation of coenzyme Q-deficient yeast by coenzyme Q analogues requires the isoprenoid side chain. *FEBS J.* **277**, 2067–2082.
- Jessen, H.J., Schumacher, A., Shaw, T., Pfaltz, A., and Gademann, K. (2011). A unified approach for the stereoselective total synthesis of pyridone alkaloids and their neurotogenic activity. *Angew. Chem. Int. Ed. Engl.* **50**, 4222–4226.
- Julien, B., Tian, Z.-Q., Reid, R., and Reeves, C.D. (2006). Analysis of the ambruticin and jerangolid gene clusters of *Sorangium cellulosum* reveals unusual mechanisms of polyketide biosynthesis. *Chem. Biol.* **13**, 1277–1286.
- Kelly, W.L., Pan, L., and Li, C. (2009). Thioesteron biosynthesis: prototype for a new family of bacteriocins. *J. Am. Chem. Soc.* **131**, 4327–4334.
- Kendrew, S.G., Katayama, K., Deutsch, E., Madduri, K., and Hutchinson, C.R. (1999). DnrD cyclase involved in the biosynthesis of doxorubicin: purification and characterization of the recombinant enzyme. *Biochemistry* **38**, 4794–4799.
- Kieser, T., Bibb, M.J., Buttner, M.J., Chater, K.F., and Hopwood, D.A. (2000). *Practical Streptomyces genetics* (Norwich, UK: John Innes Foundation).
- Kitagawa, M., Ikeda, S., Tashiro, E., Soga, T., and Imoto, M. (2010). Metabolomic identification of the target of the filopodia protrusion inhibitor glucopiericidin A. *Chem. Biol.* **17**, 989–998.
- Kroiss, J., Kaltenpoth, M., Schneider, B., Schwinger, M.G., Hertweck, C., Maddula, R.K., Strohm, E., and Svatos, A. (2010). Symbiotic *Streptomyces* provide antibiotic combination prophylaxis for wasp offspring. *Nat. Chem. Biol.* **6**, 261–263.
- Li, W., Luo, Y., Ju, J., Rajski, S.R., Osada, H., and Shen, B. (2009). Characterization of the tautomycin biosynthetic gene cluster from *Streptomyces griseochromogenes* provides new insight into dialkylmaleic anhydride biosynthesis. *J. Nat. Prod.* **72**, 450–459.
- Lipshutz, B.H., and Amorelli, B. (2009). Total synthesis of piericidin A1. Application of a modified Negishi carboalumination-nickel-catalyzed cross-coupling. *J. Am. Chem. Soc.* **131**, 1396–1397.
- Lu, H., Tsai, S.-C., Khosla, C., and Cane, D.E. (2002). Expression, site-directed mutagenesis, and steady state kinetic analysis of the terminal thioesterase domain of the methymycin/picromycin polyketide synthase. *Biochemistry* **41**, 12590–12597.
- Lu, Y., Yu, Y., Zhou, R., Sun, W., Dai, C., Wan, P., Zhang, L., Hao, D., and Ren, H. (2011). Cloning and characterisation of a novel 2,4-dichlorophenol hydroxylase from a metagenomic library derived from polychlorinated biphenyl-contaminated soil. *Biotechnol. Lett.* **33**, 1159–1167.
- Massière, F., and Badet-Denisot, M.A. (1998). The mechanism of glutamine-dependent amidotransferases. *Cell. Mol. Life Sci.* **54**, 205–222.
- Matsumoto, M., Mogi, K., Nagaoka, K., Ishizeki, S., Kawahara, R., and Nakashima, T. (1987). New piericidin glucosides, glucopiericidins A and B. *J. Antibiot.* **40**, 149–156.
- McLeod, M.P., Warren, R.L., Hsiao, W.W.L., Araki, N., Myhre, M., Fernandes, C., Miyazawa, D., Wong, W., Lillquist, A.L., Wang, D., et al. (2006). The complete genome of *Rhodococcus* sp. RHA1 provides insights into a catabolic powerhouse. *Proc. Natl. Acad. Sci. USA* **103**, 15582–15587.
- Oikawa, Y., Sugano, K., and Yonemitsu, O. (1978). Meldrum's acid in organic synthesis. 2. A general and versatile synthesis of beta-keto esters. *J. Org. Chem.* **43**, 2087–2088.
- Paget, M.S., Chamberlin, L., Atrih, A., Foster, S.J., and Buttner, M.J. (1999). Evidence that the extracytoplasmic function sigma factor sigmaE is required for normal cell wall structure in *Streptomyces coelicolor* A3(2). *J. Bacteriol.* **181**, 204–211.
- Pfeifer, B.A., Admiraal, S.J., Gramajo, H., Cane, D.E., and Khosla, C. (2001). Biosynthesis of complex polyketides in a metabolically engineered strain of *E. coli*. *Science* **291**, 1790–1792.
- Sambrook, J., and Russel, D.W. (2001). *Molecular Cloning: A Laboratory Manual* (Cold Spring Harbor, NY: Cold Spring Harbor Laboratory Press).
- Scaglione, J.B., Akey, D.L., Sullivan, R., Kittendorf, J.D., Rath, C.M., Kim, E.S., Smith, J.L., and Sherman, D.H. (2010). Biochemical and structural characterization of the tautomycin thioesterase: analysis of a stereoselective polyketide hydrolase. *Angew. Chem. Int. Ed. Engl.* **49**, 5726–5730.
- Schnermann, M.J., and Boger, D.L. (2005). Total synthesis of piericidin A1 and B1. *J. Am. Chem. Soc.* **127**, 15704–15705.
- Schnermann, M.J., Romero, F.A., Hwang, I., Nakamaru-Ogiso, E., Yagi, T., and Boger, D.L. (2006). Total synthesis of piericidin A1 and B1 and key analogues. *J. Am. Chem. Soc.* **128**, 11799–11807.

- Seco, E.M., Miranzo, D., Nieto, C., and Malpartida, F. (2010). The *pcsA* gene from *Streptomyces diastaticus* var. 108 encodes a polyene carboxamide synthase with broad substrate specificity for polyene amides biosynthesis. *Appl. Microbiol. Biotechnol.* **85**, 1797–1807.
- Shen, B., and Hutchinson, C.R. (1993). Tetracenomyacin F2 cyclase: intramolecular aldol condensation in the biosynthesis of tetracenomyacin C in *Streptomyces glaucescens*. *Biochemistry* **32**, 11149–11154.
- Surup, F., Wagner, O., von Frieling, J., Schleicher, M., Oess, S., Müller, P., and Grond, S. (2007). The iromycins, a new family of pyridone metabolites from *Streptomyces* sp. I. Structure, NOS inhibitory activity, and biosynthesis. *J. Org. Chem.* **72**, 5085–5090.
- Tago, K., Sato, J., Takesa, H., Kawagishi, H., and Hayatsu, M. (2005). Characterization of methylhydroquinone-metabolizing oxygenase genes encoded on plasmid in *Burkholderia* sp. NF100. *J. Biosci. Bioeng.* **100**, 517–523.
- Takahashi, N., Suzuki, A., and Tamura, S. (1965). Structure of piericidin A. *J. Am. Chem. Soc.* **87**, 2066–2068.
- Tanabe, M., and Seto, H. (1970). Biosynthetic studies with carbon 13. Piericidin A. *J. Org. Chem.* **35**, 2087–2088.
- Tesson, A.R., Soper, T.S., Ciustea, M., and Richards, N.G. (2003). Revisiting the steady state kinetic mechanism of glutamine-dependent asparagine synthetase from *Escherichia coli*. *Arch. Biochem. Biophys.* **413**, 23–31.
- Thompson, T.B., Katayama, K., Watanabe, K., Hutchinson, C.R., and Rayment, I. (2004). Structural and functional analysis of tetracenomyacin F2 cyclase from *Streptomyces glaucescens*. A type II polyketide cyclase. *J. Biol. Chem.* **279**, 37956–37963.
- Weber, T., Laiple, K.J., Pross, E.K., Textor, A., Grond, S., Welzel, K., Pelzer, S., Vente, A., and Wohlleben, W. (2008). Molecular analysis of the kirromycin biosynthetic gene cluster revealed  $\beta$ -alanine as precursor of the pyridone moiety. *Chem. Biol.* **15**, 175–188.
- Wendt-Pienkowski, E., Huang, Y., Zhang, J., Li, B., Jiang, H., Kwon, H., Hutchinson, C.R., and Shen, B. (2005). Cloning, sequencing, analysis, and heterologous expression of the fredericamycin biosynthetic gene cluster from *Streptomyces griseus*. *J. Am. Chem. Soc.* **127**, 16442–16452.
- Wietzorrek, A., and Bibb, M. (1997). A novel family of proteins that regulates antibiotic production in *streptomycetes* appears to contain an OmpR-like DNA-binding fold. *Mol. Microbiol.* **25**, 1181–1184.
- Xu, W., Cai, X., Jung, M.E., and Tang, Y. (2010). Analysis of intact and dissected fungal polyketide synthase-nonribosomal peptide synthetase *in vitro* and in *Saccharomyces cerevisiae*. *J. Am. Chem. Soc.* **132**, 13604–13607.
- Zhang, W., Ames, B.D., Tsai, S.-C., and Tang, Y. (2006). Engineered biosynthesis of a novel amidated polyketide, using the malonamyl-specific initiation module from the oxytetracycline polyketide synthase. *Appl. Environ. Microbiol.* **72**, 2573–2580.
- Zhang, W., and Tang, Y. (2009). *In vitro* analysis of type II polyketide synthase. *Methods Enzymol.* **459**, 367–393.